



STRUCTURAL SCIENCE
CRYSTAL ENGINEERING
MATERIALS

Volume 76 (2020)

Supporting information for article:

**Effect of growth modes on electrical and thermal transport of
thermoelectric ZnO:Al films**

**Shiying Liu, Guojian Li, Mingdi Lan, Yongjun Piao, Koji Miyazaki and
Qiang Wang**

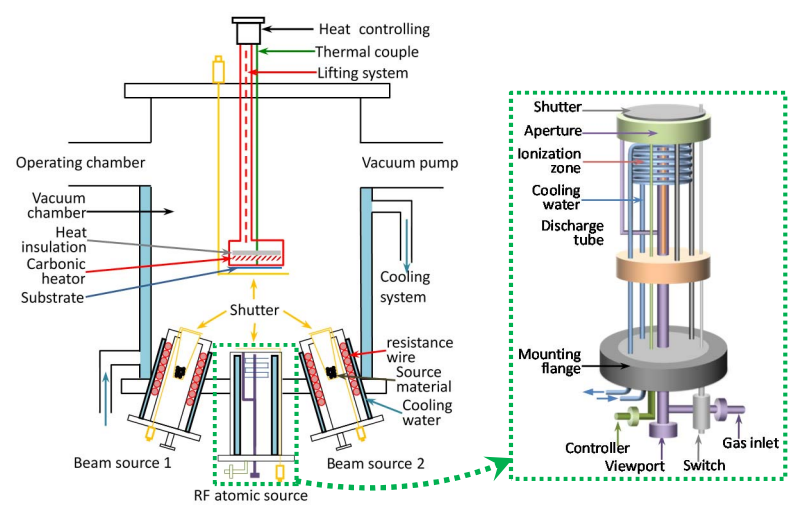


Fig. S1 Schematic diagram of vacuum thermal evaporation assisted by RF atomic source

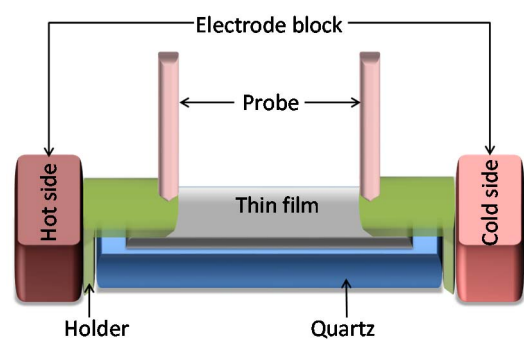


Fig. S2 Schematic diagram of sample holder for the resistivity and Seebeck coefficient measurement in the ZEM-3 equipment (Liu et al, 2018).

Table S1 Hall voltages of ZnO:Al films with the constant magnetic field of 0.558 T

Substrate temperature	AC(mV)	-AC(mV)	BD(mV)	-BD(mV)	Average
RT	1.0387	-0.9997	1.0353	-1.0032	1.019
300°C	1.5378	-1.4829	1.5155	-1.5001	1.509
450°C	9.1944	-9.1399	9.1943	-9.1431	9.168
600°C	21.5566	-21.2852	21.4698	-21.3792	21.423

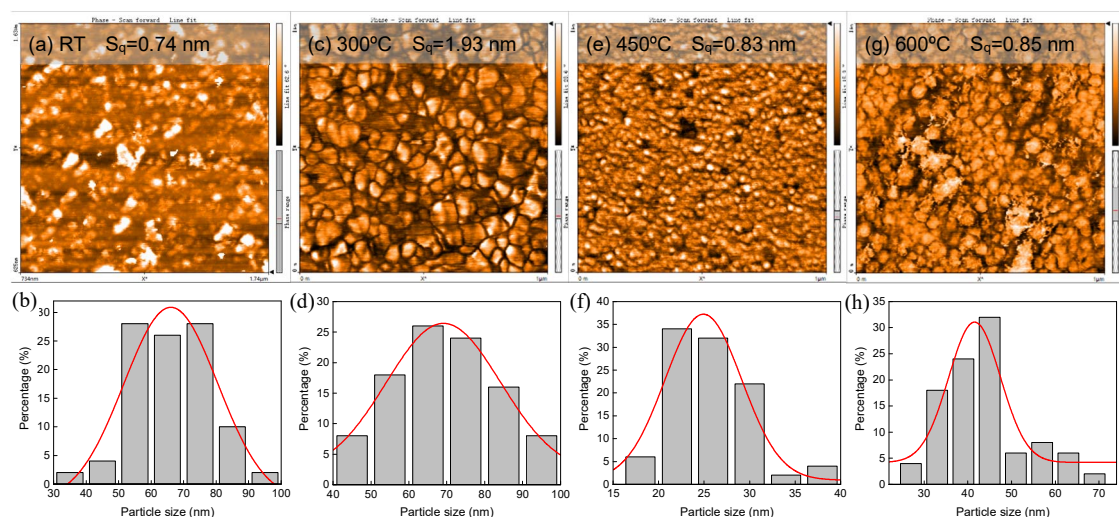


Fig.S3 AFM phase-contrast images (upper half) and particle size distribution (lower half) of ZnO:Al films at different substrate temperatures

The protruding particle is sparse but larger (66 ± 31.18 nm) on RT film with a smaller surface roughness ($S_q = 0.74$ nm). Spherical-shape particles (69.5 ± 28.47 nm) distribute uniform on 300°C film with a surface roughness of 1.93 nm. The surface roughness is 0.83 nm and 0.85 nm at the substrate temperature of 450°C and 600°C respectively. The particle size on 450°C film is smaller (24.85 ± 8.51 nm) while the particle size on 600°C film is 41.55 ± 27.53 nm.

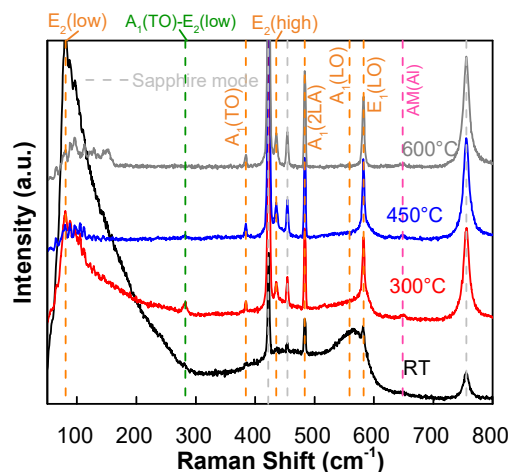


Fig.S4 Raman spectra of ZnO:Al films at different substrate temperatures

In the wurtzite ZnO structure, first-order vibration of the optic modes obeys the existence $\Gamma_{\text{opt}} = A_1 + 2B_1 + E_1 + 2E_2$. Polar optical vibration in the lattice consists of transverse and longitudinal direction ($A_1(\text{TO})$ and $A_1(\text{LO})$). Two-dimensional E_1 mode split into transverse optical (TO) and longitudinal optical (LO) modes. The presence of $E_2(\text{low})$ mode associated

with the vibration of Zn atoms and $E_2(\text{high})$ mode of oxygen atoms in ZnO films. The peaks observed at 80 cm^{-1} , 435 cm^{-1} correspond to the $E_2(\text{low})$ and the $E_2(\text{high})$ modes respectively. The transverse vibration of polar mode located at 384 cm^{-1} is the phonon confinement vibration induced by native defects of ZnO films which is resulted from oxygen vacancies. The acoustic vibration of ZnO films cause a shape $A_1(2\text{LA})$ peak at 483 cm^{-1} . The increase of micro-stress and carrier scattering can be achieved by vibration. Carrier mobility of ZnO:Al film shows the higher value at RT substrate temperature, the 600°C film exhibits the lower carrier mobility. The optical vibration of ZnO films at 560 cm^{-1} and 582 cm^{-1} attribute to vibration peaks of $A_1(\text{LO})$ and $E_1(\text{LO})$, caused by impurities and defects in ZnO:Al films. The anisotropy of ZnO:Al films can be also presented indirectly. $A_1(\text{LO})$ mode is parallel to the c-axis orientation and $E_2(\text{LO})$ mode is to the surface atom of substrate. Besides, the additional modes at 649 cm^{-1} is caused by Al dopant. The peak at 283 cm^{-1} on 300°C film attributes to the second-order $[A_1(\text{TO})-E_2(\text{low})]$ vibration mode, caused by the unstable of polar and split vibration.

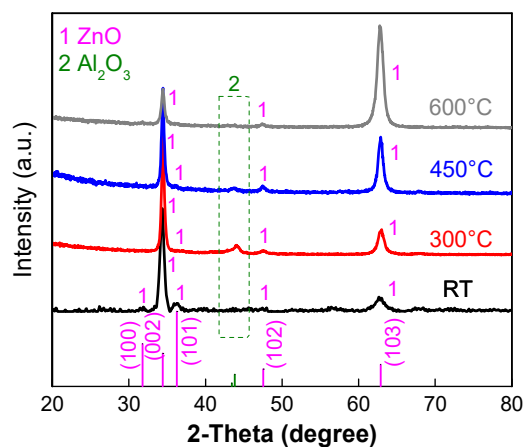


Fig.S5 XRD patterns of RF-assisted evaporated ZnO:Al films at different substrate temperatures.

An increase in substrate temperature results in the decrease of diffraction peak of ZnO (002) facet and gradual increase of (103) facet. The index M is to describe the texture coefficient of each planes:

$$M = \frac{I_{(h_0k_0l_0)} / \sum I_{(hkl)}}{I_{0(h_0k_0l_0)} / \sum I_{0(hkl)}}$$

where I_0 is the standard XRD intensity and I is the experimental data. \sum is the sum of the intensities of the peaks for (110), (002), (001), (102) and (103) planes. The direction with the highest intensity of the (002) facet on RT film is $M_{(002)}=3.39$. The index $M_{(002)}$ of ZnO:Al films

gradually decrease to 1.83, 1.38, 0.45 respectively with the substrate temperature increase to 300°C, 450°C and 600°C. Meanwhile, the index $M_{(103)}$ of (103) facet are 0.31, 0.47, 1.08 and 2.38 respectively as the substrate temperature increase from RT to 600°C.

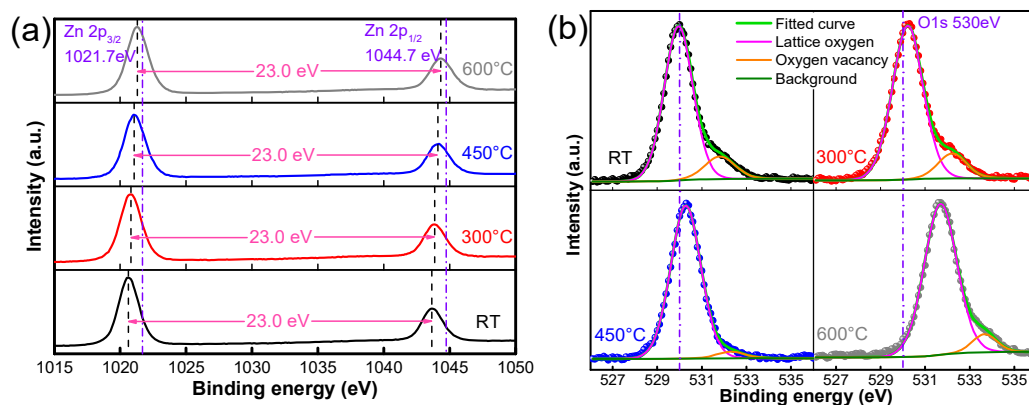


Fig. S6 High-resolution XPS spectra of O 1s (a) and Zn 2p (b) of ZnO:Al films at different substrate temperatures

High-resolution XPS spectra can be used to analyze the chemical states and native defects of ZnO:Al films. The Zn 2p spectra for the ZnO:Al films consist of two peaks, identified as Zn 2p_{3/2} and Zn 2p_{1/2}. The binding energy difference of two peaks is 23.0 eV, as shown in Fig. S6(a). This chemical state of Zn is the same with ZnO. That is, the ZnO:Al film fabricated is the ZnO phase. The binding energy of O1s peak in ZnO:Al film at RT is 529.9 eV. The binding energy of Zn2p and O1s increases with the increase of substrate temperature. Furthermore, the O1s of ZnO:Al films are asymmetric peak which can be divided into two peaks of lattice oxygen and oxygen vacancies (V_O), as shown in Fig. S6(b). Content of V_O is expressed by the peak area. The concentrations of V_O are 13.48%, 13.00%, 3.76% and 8.25%, respectively at the substrate temperature of RT, 300°C, 450°C and 600°C.